Hydrogeochemical characteristics of the groundwater in the quaternary aquifer of western fringes of El-Minia Governorate, Egypt using an integration of geochemical modeling and geo-statistical techniques

Esam Ismail[a,*], Rafat Zaki[a], Nada Rapantova[b], Monika Licbinska[b], Haiaa Sharawi[a]

[a]*Department of Geology, Faculty of Science, Minia University, Minia 61519, Egypt, Tel. +20 1025511886;*
emails: essam.ismail@mu.edu.eg (E. Ismail), zakirafat1@yahoo.com (R. Zaki), haiaasharawi79@gmail.com (H. Sharawi)
[b]*VSB – Technical University of Ostrava, 17. listopadu 15, 708 33 Ostrava, Czech Republic,*
emails: nada.rapantova@vsb.cz (N. Rapantova), monika.licbinska@vsb.cz (M. Licbinska)

ABSTRACT

Groundwater is a very important source of drinking and irrigation water especially in areas with little to no surface water sources. In the western desert of Egypt, groundwater acts as the main source of irrigation in the new reclamation project. The authors of the article used major constituents and trace elements chemistry as well as bacteriological and biological water analysis to assess the hydrogeochemical characteristics in the western bank of the River Nile, West El-Minia District. In order to fulfill the scope of work for this study, 88 groundwater samples were collected from the Pleistocene aquifer which represents the main aquifer in the study area. The groundwater samples were analyzed for pH, electrical conductivity (EC), total dissolved solids (TDS), major cations (Ca^{2+}, Mg^{2+}, Na^+, K^+), major anions (HCO_3^-, SO_4^{2-} and Cl^-) and trace metals (Mn, Cu, Pb, Zn, Ni, Co, As, Hg, Se, Al, Cd, Cr, B, and Fe). Microbiological and microscopic studies of the collected water samples were carried out to determine the micro-organisms' in order to confirm the safety of the water for human consumption. Also, statistical analysis and hydrogeochemical modeling were used to interpret the collected data. The study revealed that in all the collected water samples, alkaline earth metals have values higher than alkalies and are of meteoric origin. The groundwater chemistry is mainly controlled by rock weathering with a secondary contribution from anthropogenic sources. Forty-nine percent (49%) of analyzed water samples have trace constituents above the recommended limits for water use for drinking and irrigation purposes. The highest linear correlation was shown between TDS and EC, HCO_3, Na^+, K^+, Ca^{2+} and Mg^{2+}, all macro-components and chlorides, between boron and chrome, as well as cobalt and lead. All sampled waters were classified as Ca-HCO_3 water type and calcite precipitate in all collected water samples.

Keywords: Hydrogeochemistry; West El-Minia; Major elements constituents; Trace elements; Statistical analysis; Hydrogeochemical modeling

1. Introduction

Groundwater is one of the most valuable natural resources supporting human health, economic development, and ecological diversity. Groundwater has become a very important and dependable source of water in all climatic regions, including both urban and rural areas of developed and developing countries [1], because of its inherent qualities (e.g., consistent temperature, widespread and continuous availability, excellent natural quality, limited vulnerability,

---

* Corresponding author.

low development costs, drought reliability, etc.) [2]. Due to the persisting, a sharp rise in population growth and agricultural activity representing the economic foundation in Egypt, the need to develop and manage water resources has become a more urgent matter than before.

The study area is located along the western bank of the Nile Valley facing El-Minia Governorate and lies between latitudes 27°35 and 28°45′N and longitudes 30°30′ and 31°10′ E (Fig. 1). The study area is characterized by long, hot summers, cold winters, and rare rainfall. Furthermore, the average air temperature is about 36.8°C in summer and 10.5°C in winter and the relative humidity in summer is higher than in winter and varies between 36% and 61% [3]. As for the area's monthly evapotranspiration, it ranges from 3.2 mm/d in January to 10.0 mm/d in June, and the evaporation loss from the water distribution system varies from 2.2 mm/d in

January to 8.6 mm/d in June [4]. The hydrogeological and hydrogeochemical conditions of the West Nile Valley of El-Minia Governorate and its surroundings have been studied by many authors, including [5–17].

For the related studies conducted in Egypt, El-Sayed et al. [5] studied the hydrochemical characteristics and evolution of groundwater and surface water in the western part of the River Nile, El-Minia district. El Kashouty [6] reported that the groundwater chemical composition was controlled by different factors such as aquifer lithology, climate, topography, precipitation, and land use application such as agricultural and industrial activities. Morsi [7] studied the environmental impact of anthropogenic activities on surface and groundwater systems in the western part of the River Nile of El-Minia district. Ismail [8] used hydrochemical, geophysical and remote sensing studies to delineate and
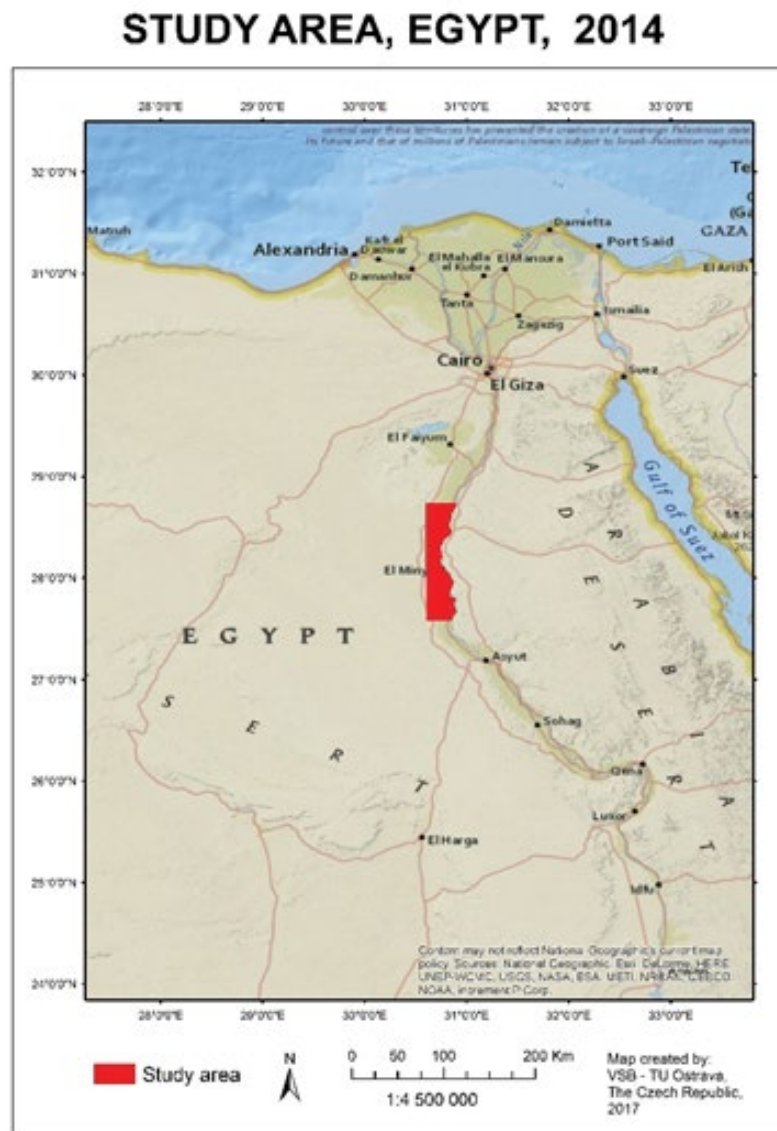
Fig. 1. Location map of the study area.

evaluate Pleistocene aquifer in the west Tahta area. Zaki et al. [9] studied the impact of surface and groundwater pollutions on irrigated soil in west El Minia. Ismail et al. [10] evaluated the groundwater suitability for irrigation and drinking purposes in the west El-Minia district based on the major ions and studied the characteristics of groundwater potentialities in West Nile Valley, south of Minia Governorate, Egypt. Ismail and El-Rawy [13] assessed the hydrochemistry characteristics of groundwater resources in West Sohag, Egypt and evaluated it for different uses. Abdelhalim et al. [14] developed a numerical groundwater flow model for the Quaternary aquifer in Samalut city, Minia Governorate, Egypt. Farag et al. [15] studied the hydrochemical characteristics and chemically evaluated the water resources in El-Minia Governorate for drinking and irrigation. El-Rawy et al. [16] used geographic information system,, hydrogeochemistry, and factor statistical analysis to assess the groundwater quality in Qena Governorate, Egypt. Snousy et al. [17] studied trace element occurrence and distribution problems in the irrigation water at El-Minia district, north Upper Egypt.

About international research, many authors such as [18–21] studied the characteristics of groundwater and evaluated it for different purposes. Yasmin et al. [18] evaluated the quality of groundwater in the Barisal district of Bangladesh for both irrigation and drinking purposes. Rasul [19] assessed the water quality of the Derbendikhan Reservoir by identifying the critical parameters affecting the water chemistry and its variation. They further determined the spatial distribution and concentration of major cations and anions, evaluated the usability of this reservoir for drinking, agriculture, and other purposes. Rasul [19] also discussed possible contamination and changes in water characteristics over time by comparing the obtained results with those of previous studies. Li et al. [20] assessed the water quality status and identified the hydrochemical processes contributing to the dissolved constituents of the water in the Guohua phosphorite mine, Guizhou Province, China. For the Guohua phosphorite mine assessment, multivariate statistical techniques and correlation analysis were used to employ a better understanding of the hydrogeochemical processes. Moreover, they evaluated water quality for domestic and irrigation purposes, assessed the geochemistry and quality of groundwater in the Hongdunzi coal mining area in northwest China. They also investigated the mechanisms governing the coal mining area hydrogeochemistry and the hydraulic connectivity between adjacent aquifers.

In the area under investigation, heavy and bacteriological analysis in groundwater has not been used by any study prior. In the present study, the heavy and trace metals, as well as bacteriological and biological water analysis, were used to detect the characteristics and evaluate the groundwater for different purposes, mainly drinking and irrigation. The groundwater quality assessments were carried out by evaluating the physicochemical parameters such as pH, electrical conductivity (EC), total dissolved solids (TDS), Ca^{2+}, Mg^{2+}, Na^+, K^+, HCO_3^-, Cl^-, SO_4^{2-}, heavy and trace metals (Pb, Cu, Cd, Cr, Se, Co, Zn, As, Hg, Ni, Al, and Fe), in addition to the bacteriological and biological water analysis. The statistical analysis and hydrogeochemical modeling for interpreting the collected data were used in this study.

2. Materials and methods

This study is based on an extensive field campaign performed in the area of interest located along the western bank of the Nile Valley facing El-Minia Governorate. The study area covers a surface area of 4,350 km². Eighty-eight (88) groundwater samples (Fig. 2) were collected from wells after a pumping period of at least 1 h and were filtered through >0.45 μm nucleopore membrane and transferred into cleaned polyethylene bottles. The geographic coordinates and ground elevation of water points were measured using the Global Positioning System model. The temperature, pH, TDS and EC was measured immediately after sampling (in-situ) by the Ultrameter SM101 instrument. The data on groundwater level, depth to water and total depth of drilling for each point were collected by the assistance of the wells' owners. The chemical analyses and bacteriological tests were carried out at the Central Health Laboratories, Abdein, Cairo, Egypt, using the standard methods adopted by the American Public Health Association [22] and the results are shown in Table 1. Calcium (Ca^{2+}), magnesium (Mg^{2+}), bicarbonate (HCO_3^-) and chloride (Cl^-) were analyzed by volumetric titration methods, sodium (Na^+) and potassium (K^+) were measured using a flame photometer, and sulfate (SO_4^{2-}) was determined by UV spectrophotometer.

To validate the quality of water analyses, charge balance error (CBE) was computed. Water samples having a higher
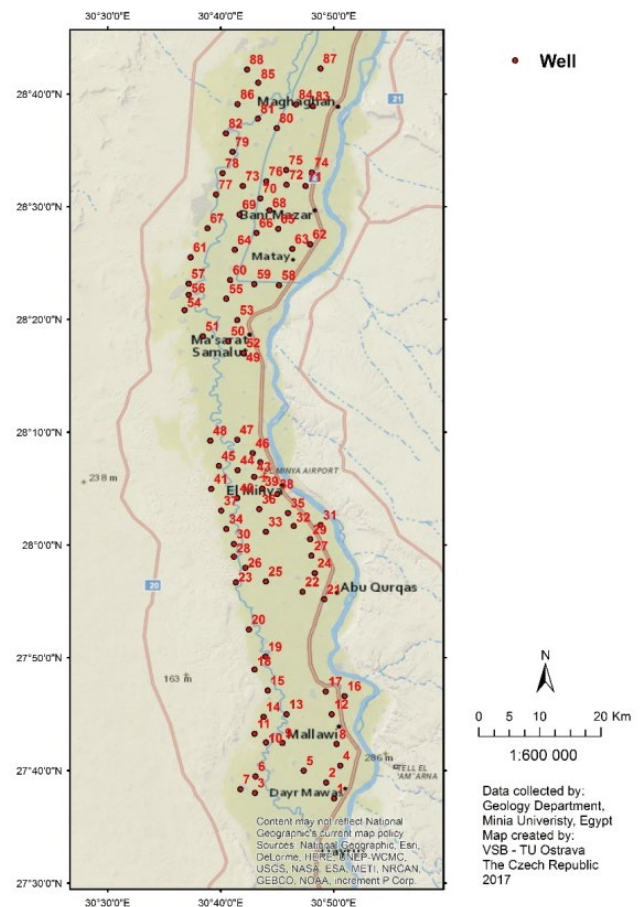
Fig. 2. Well location map of the studied groundwater samples.

Table 1
Statistics of chemical parameters (all in mg/L and EC in µs/cm)

Parameters	PH	TDS	EC	Ca^{2+}	Mg^{2+}	Na^+	K^+	HCO_3^-	SO_4^{2-}	Cl^-
Average	7.88	507.89	763.05	52.86	24.76	29.88	3.92	299.52	11.15	32.61
Median	7.90	495.00	743.00	48.00	23.70	28.00	3.20	290.00	10.00	32.50
Variance	0.04	39,877.71	89,806.02	480.74	105.59	95.15	4.19	12,144.17	21.38	122.36
Standard deviation	0.21	199.69	299.68	21.93	10.28	9.75	2.05	110.20	4.62	11.06
Minimum	6.80	210.00	316.00	21.60	9.00	19.00	2.00	138.00	4.00	15.00
Maximum	8.20	1,460.00	2,193.00	150.00	74.00	82.00	12.00	850.00	22.00	70.00

concentration of cations show positive CBE, while negative CBE is credited to higher concentrations of anions [23]. CBE was computed by using the following equation

$$CBE = \frac{\left[\sum cations - \sum anions\right]}{\left[\sum cations + \sum anions\right]} \times 100 \quad (1)$$

In the equation, ionic concentrations are expressed in milli-equivalent per liter (meq/L).

According to the standard protocols, only these water samples with <5% CBE were accepted [24]. The acidification was accomplished in situ and case of determination of toxic metals, the samples were stored in a refrigerator at approximately 20°C to prevent changes in volume due to evaporation. The heavy and trace metals, that is, Pb, Cu, Cd, Cr, Se, Co, Zn, As, Hg, Ni, Al, and Fe were determined by atomic absorption spectrometer (GBC, GF 3000, USA). If the value of the sample is below the limit of quantification 9LOQ), some analyst's use 0, others use the LOD itself, and others split the difference and use half of the LOD. For the purposes of this study, the limit of detection (LOD) itself is used. The results were evaluated following the water quality standards given by [25,26].

Descriptive and multivariate statistics of hydrogeochemical data were computed and calculated using UNISTAT software (https://www.unistat.com/). A microbiological procedure and microscopic study of the collected water samples were carried out to determine the micro-organisms to confirm safety for human consumption. The bacteriological test involved making serial dilutions of the sample (1–10, 1–100, 1–1,000, etc.), in sterile water and cultivating these on nutrient agar in a dish that was sealed and incubated. The typical media included plates count agar for a general count or MacConkey agar to count gram-positive bacteria, such as *E. coli*. Typically, one set of plates was incubated at 22°C for 24 h and a second set at 37°C for 24 h. The composition of the nutrient usually included reagents that resist the growth of non-target organisms and make the target organism easily identified, often by a color change in the medium. Some recent methods include a fluorescent agent so that the counting of the colonies can be automated. At the end of the incubation period, the colonies were counted by eye, which was a short procedure.

Hydrogeochemical modeling was carried out using PHREEQC [27], a modeling tool used to understand hydrogeochemical stability and processes taking place in the saturated part of an aquifer. Conclusions and recommendations concerning future monitoring programs were then drawn.

2.1. Geological and hydrogeological setting of study area

The studied area is overlain by sedimentary rocks that range in age from the Middle Eocene to Holocene. According to [28], the lithostratigraphic succession of the study area is composed, from base to top, of the following rock units, (Fig. 3):

- *Eocene rocks*: the area is formed of a thick sequence of Middle Eocene fossiliferous limestone with some layers of sandy, chalky and marly intercalation [29]. The Middle Eocene rocks mainly making up the limestone plateau that is found in the west part of the study area.
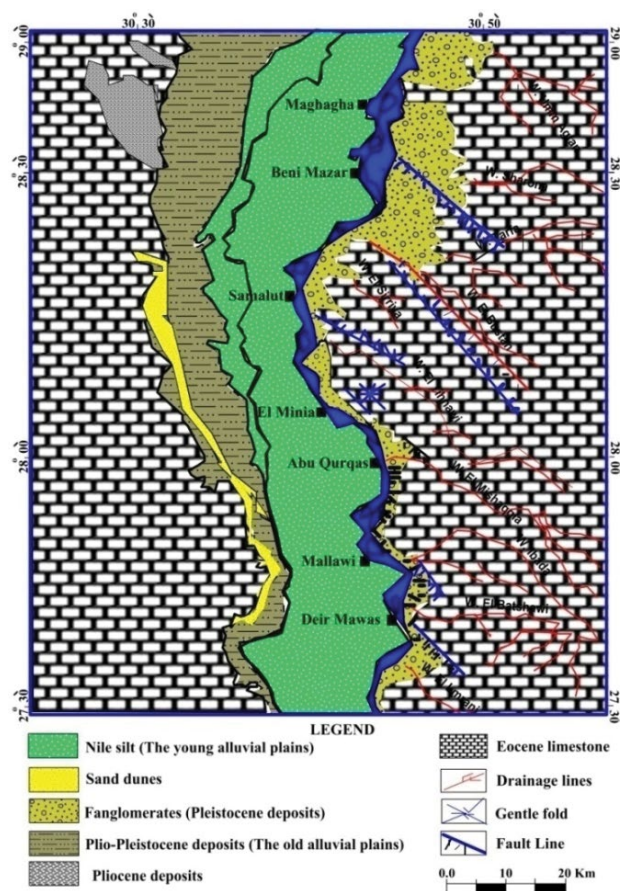
Fig. 3. Geologic map of the study area and its vicinities.

- *Pliocene deposits*: are exposed in the northwestern part of the study area and represented by dark-colored clays interbedded with sandstone lenses and act as the base of the Pleistocene aquifer.
- *Plio-Pleistocene deposits*: these deposits constitute the earliest types of deposits laid by the Nile and form Pre-Nile terraces. In the subsurface, Plio-Pleistocene deposits (undifferentiated sands and gravels) were reported by [30] in some deep-water wells in the area between Samalut and El-Minia.
- *Pleistocene deposits*: are composed of massive cross-bedded fluvial sand with gravel and clay intercalate. This unit represents the main water-bearing formation in the study area.
- *Holocene deposits*: comprise all series of unconsolidated sediments, accumulated under different environmental conditions (Nile silts and sand dunes).

Hydrogeologically, the Quaternary aquifer represents the main aquifer in the study area. It is a semi-confined aquifer composed of gravels and sands. This aquifer lies directly on the Pliocene clay, which acts as the impermeable base of the aquifer (aquiclude) and the fissured Eocene limestone (Fig. 4) [31].

Generally, the thickness of this aquifer decreases towards the Eocene plateau and is hydraulically connected with the underlying aquifer (Eocene) through the faults. The main source of recharge to the Quaternary aquifer is mainly from surface water (River Nile and irrigation canals). The water discharge of this aquifer is through the evaporation process as well as the connection to the underlying aquifer and river. The depth to the groundwater (water table) of the Quaternary aquifer ranges from 0.9 to 8 m (Fig. 5) and the water level ranges between 29.4 m in the northern part and 43 m in the southern part of the study area. The groundwater level declines from the southwest to northeast direction with a variable hydraulic gradient. The level is affected by the hydraulic potentials of the surface water in the irrigation and drainage system. The main groundwater flow direction in the study area is from the southwest to the northeast towards the River Nile (Fig. 6).
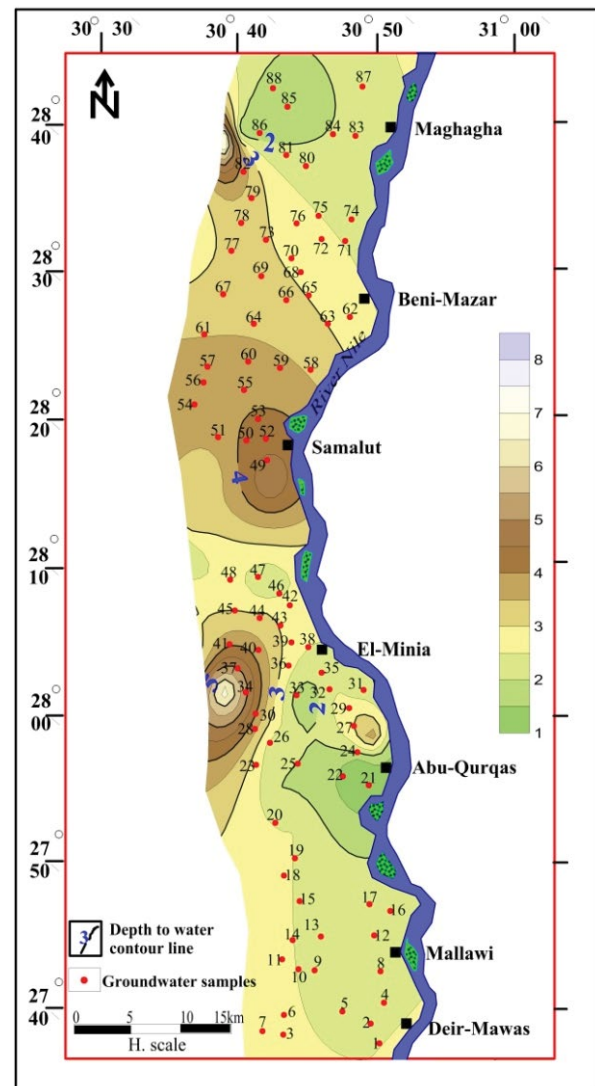
Fig. 5. Depth to water contour map.
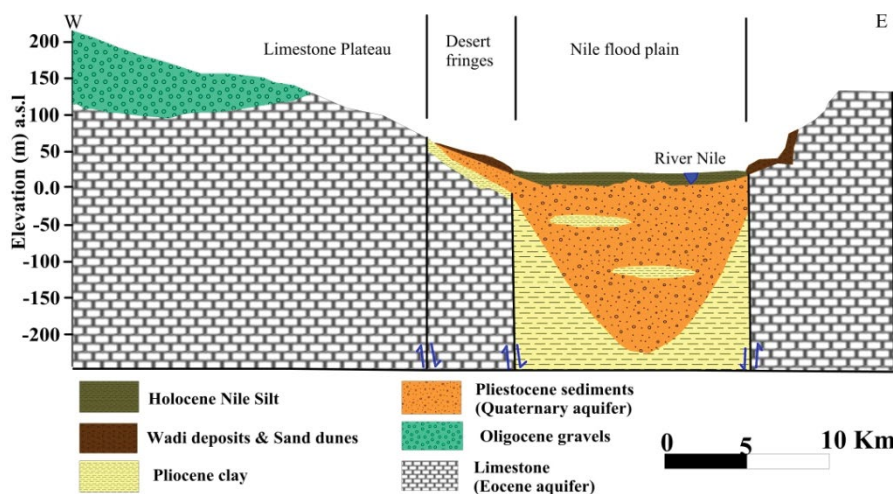
Fig. 4. General hydrogeological cross-section in El-Minia area after [25].

3. Results and discussion

3.1. Hydrogeochemical classification

Based on the collected data set, the researcher was able to describe the hydrogeochemical state of groundwater to better understand natural hydrogeochemical processes and to distinguish potential anthropogenic impacts. The improved knowledge could contribute to the assessment of potential use of groundwater in the region, strategy of groundwater quality and quantity protection including monitoring programs.

3.2. Ion chemistry

The pH in the groundwater depends mainly on the composition of the rock and sediment through which the water flows. In the analyzed water samples, pH values range between 7.6 and 8.2 with an average of 7.9 within the permissible limits of Egyptian standards guidelines for drinking water, 2007. EC of groundwater samples collected from the Pleistocene aquifer varies in a wide range from 316 to 2,193 μs/cm with an average of 1,255 μs/cm. The EC contour map (Fig. 7) shows a gradual increase in conductivity toward the southern and western parts of the area due to the leaching and dissolution of the limestone present in the west of the study area. The TDS of the collected groundwater samples varies from 212 to1,460 mg/L with an average of 836 mg/L. 98% of samples that have TDS less than 1,000 mg/L can be classified according to [32] as freshwater. Only 2% of the groundwater samples are slightly saline (Table 2). The salinity contour map of the study area (Fig. 8) shows an increase in salinity from the east to the west, which reflects the impact of the leaching effect on the limestone in the western part. Additionally, this is due to the low River Nile recharge and agricultural wastewater leaching in these parts.
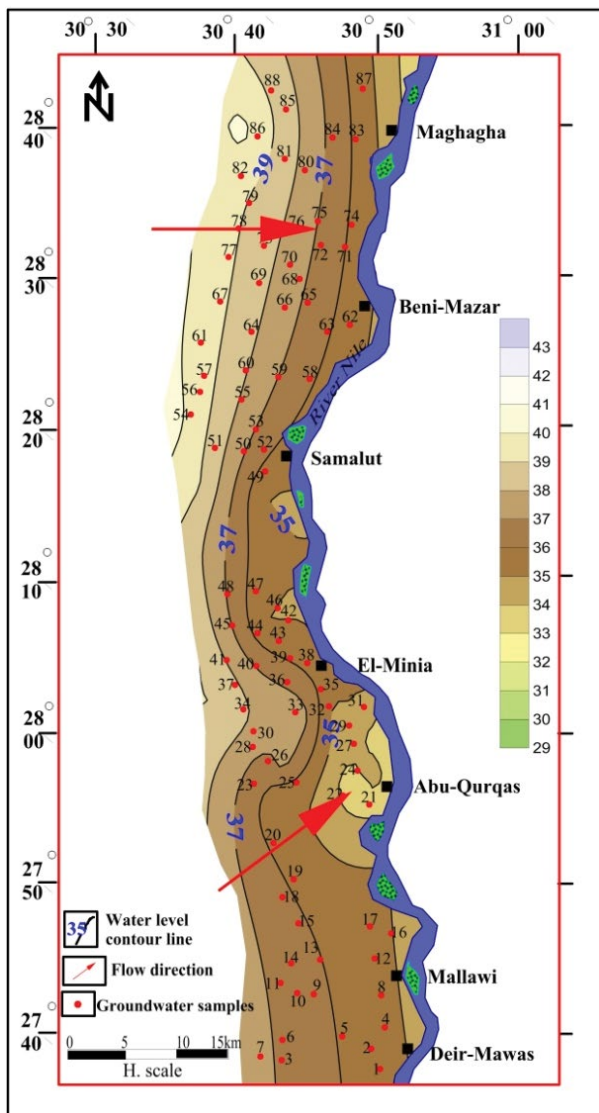
Fig. 6. Water level contour map.
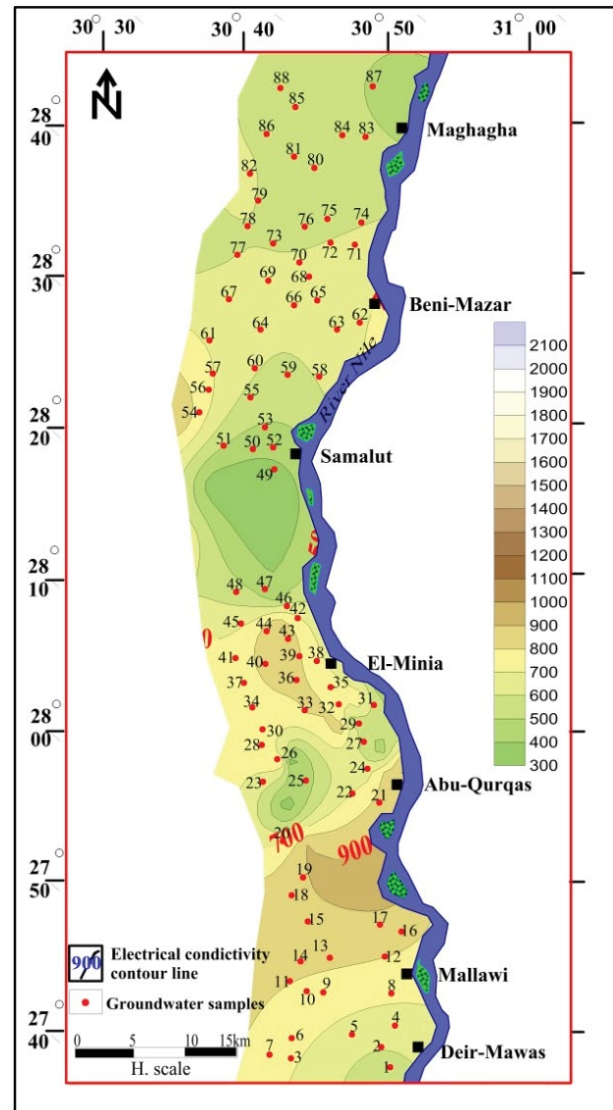
Fig. 7. EC contour map.

The collected groundwater samples have total hardness (TH) values varying from 145 to 680 mg/L with an average of 413 mg/L. Furthermore, 90% of the analyzed water samples fall within the very hard category (according to [32]) and 10 % in the hard category (Table 3). The high values of TH are attributed to the leaching and dissolution processes of calcium and magnesium-bearing deposits.

The concentration range of major cations and major anions of the analyzed groundwater samples falls within the acceptable range of the World Health Organization (WHO) [25]. In the study area, the concentration of calcium ranges between 21.6 and 150 mg/L, with an average of 52.86 mg/L. The high value of calcium is due to the weathering of calcium-bearing rocks such as limestone. The concentration

Table 2
Hem salinity classification of collected groundwater samples

Water type	TDS	Studied samples%
Fresh water	<1,000 mg/L	86 samples 98%
Slightly saline	1,000–3,000 mg/L	2 samples 2%
Moderately saline	3,000–10,000 mg/L	–
Very saline	10,000–35,000 mg/L	–
Brine	>35,000 mg/L	–

Table 3
Hem water hardness classification

Water type	Classification	Studied samples%
Soft	0–60 mg/L as $CaCO_3$	
Moderately	61–120 mg/L as $CaCO_3$	
Hard	121–180 mg/Las $CaCO_3$	9 samples 10%
Very hard	>180 mg/L as $CaCO_3$	79 samples 90%
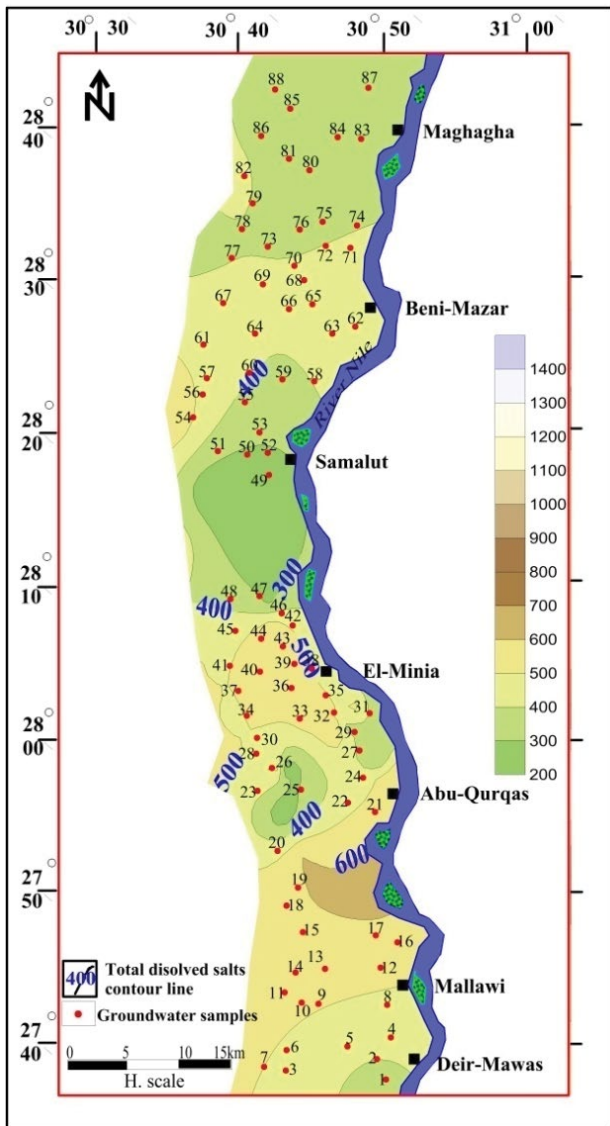
Fig. 8. Total dissolved salts contour map.
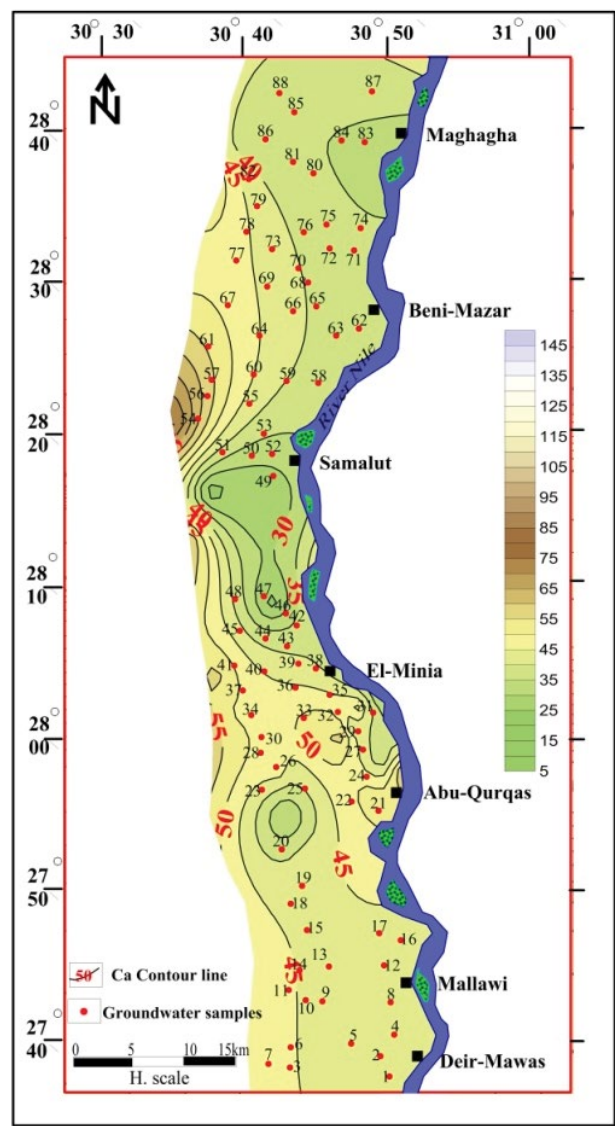
Fig. 9. Spatial distribution of Ca²⁺ ion.

of magnesium varies from 9 to 74 mg/L, with an average of 24.76 mg/L. The concentration of sodium ranges from 19 to 82 mg/L with an average of 29.88 and the concentration of potassium varies between 2 to 12 with a mean average of 3.92 mg/L. The concentration of anions in the groundwater samples shows that bicarbonate concentration varies from 138 to 850 with an average of 299.52 mg/L. The high concentration of HCO_3^- is attributed to agricultural return flows where dissolved carbonate minerals are precipitated in the soil due to evaporation, in addition to the recharge from surface water. The concentration of chloride ranges between 15 and 70 mg/L with an average of 32.61 mg/L, while the concentration of sulfate varies from 4 to 22 mg/L with an average of 11.21 mg/L. The distribution maps of major cations and major anions (Figs. 9–15) show that high values are present in the western part of the study area and low values are in the eastern part. This reflects the increase in the westerly direction that corresponds to a TDS increase trend.

The heavy metals in the collected groundwater samples show that 49% of the samples exhibit high concentrations values of B (0.0024–1.867ppm), Cd (0.0001–0.18 ppm), Mn (0.1–1.6 ppm). The samples also exhibits high concentrations value of As (0.001–0.245 ppm), Cr (0.0007–0.3212 ppm), Ni (0.001–0.245 ppm), Co (0.001–1.40 ppm), Pb (0.0001–0.365 ppm), and Se (0.001–0.294 ppm) (Table 4). The high values result from anthropogenic activities, such as industrial wastewater recharged from El Moheet drain, drainage water of splendiferous irrigated soil and Eocene rocks, extensive use of fertilizers as well as corrosion of the well casing and other pipes.

3.3. Bacteriological content

Bacteriological and biological analyses of the collected water samples show that 75% are free from Protozoa, Schistosoma, Minthe, and Charophyte (Algae) as well as
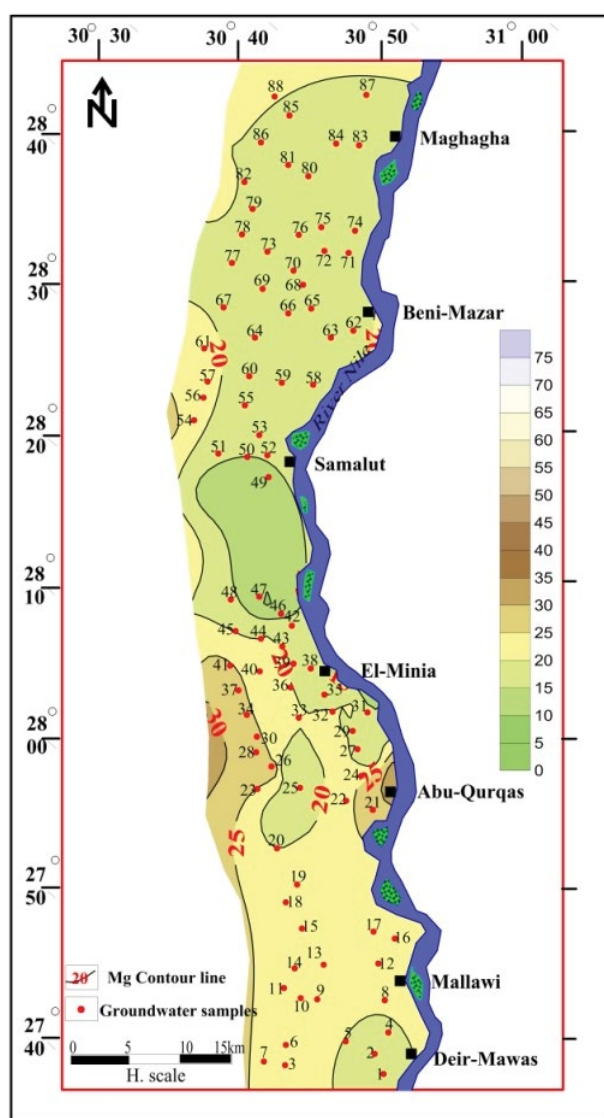
Fig. 10. Spatial distribution of Mg^{2+} ion.
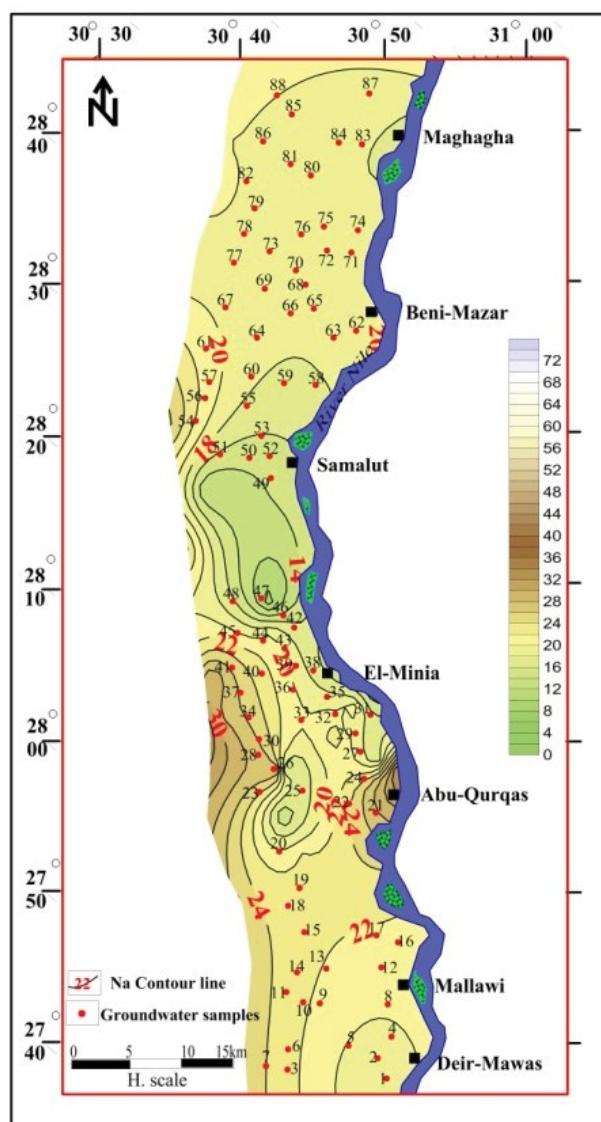
Fig. 11. Spatial distribution of Na^+ ion.
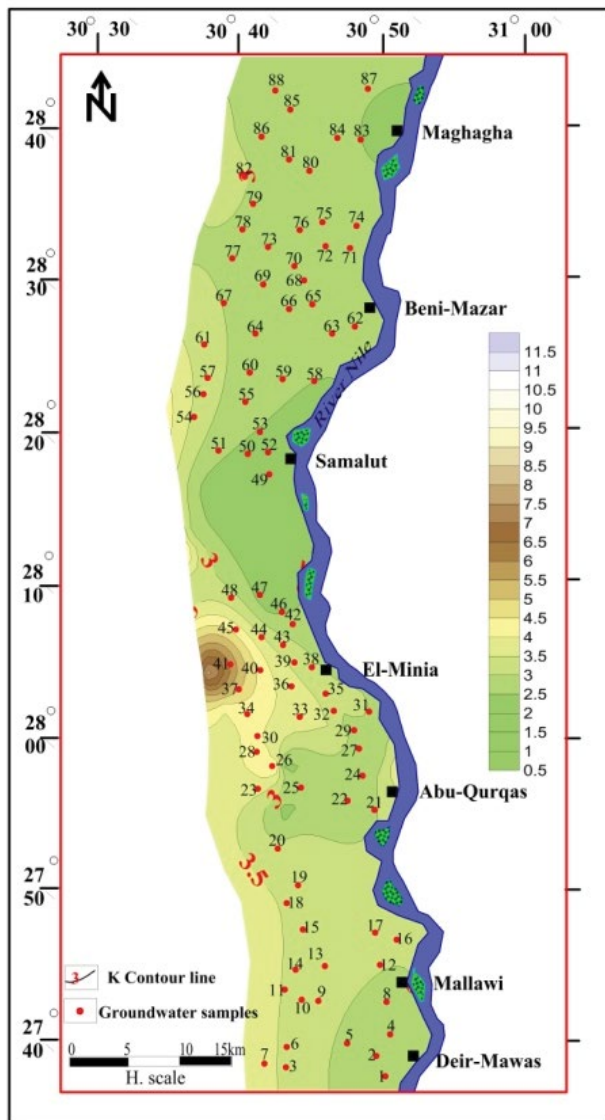
Fig. 12. Spatial distribution of K$^+$ ion.

Fig. 13. Spatial distribution of HCO$_3^-$ ion.

negative gram bacteria. On the other hand, 25% of the collected samples are positive (shows the presence of bacteria), due to infiltration from septic tanks.

3.4. Groundwater origin

After presenting the chemical data of the collected groundwater samples on a Piper diagram [33], it was found that all the samples fall into no dominant, Ca field class in the cationic triangle and they fall into no dominant field in the anionic triangle. All the collected samples fall into the class (1) of a diamond-shaped central field (Fig. 16), which reveals that, in all analyzed water samples, alkaline earth metals (Ca^{2+} + Mg^{2+}) exceed alkali metal cations (Na$^+$ + K$^+$) and that they are of meteoric origin.

The main natural processes that control groundwater chemistry are atmospheric precipitation, rock weathering, evaporation, and fractional crystallization. According to [34],

the groundwater sample ratios of (Na$^+$ + K$^+$):(Na$^+$ + Ca^{2+} + K$^+$) have been plotted against TDS, the ratio of Cl$^-$:(Cl$^-$ + HCO$_3^-$) has similarly been plotted against TDS and is shown in (Fig. 17). This figure proves that most of the samples suggest that the chemical weathering of rock-forming minerals affects the groundwater quality during the dissolution of the host rock.

3.5. Statistical analysis of data

Hydrogeochemical data were subjected to a statistical analysis by which the probability distribution of specific data series has been determined. The analysis was performed by using the UNISTAT software ((https://www.unistat.com/) and has proved that the parameters best correspond to the lognormal distribution. This fact has been reflected in the geo-statistical analysis. Also, a multi-parametric principal component analysis (PCA) was elaborated [35] and these results are evident in Fig. 18. The set is relatively homogenous, and the
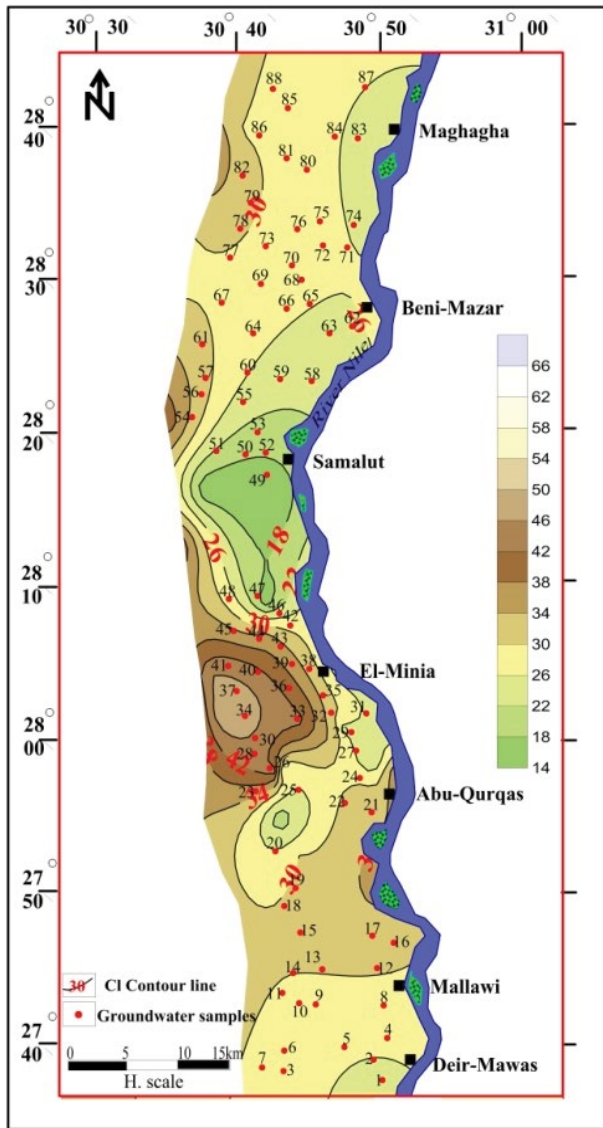
Fig. 14. Spatial distribution of Cl⁻ ion.
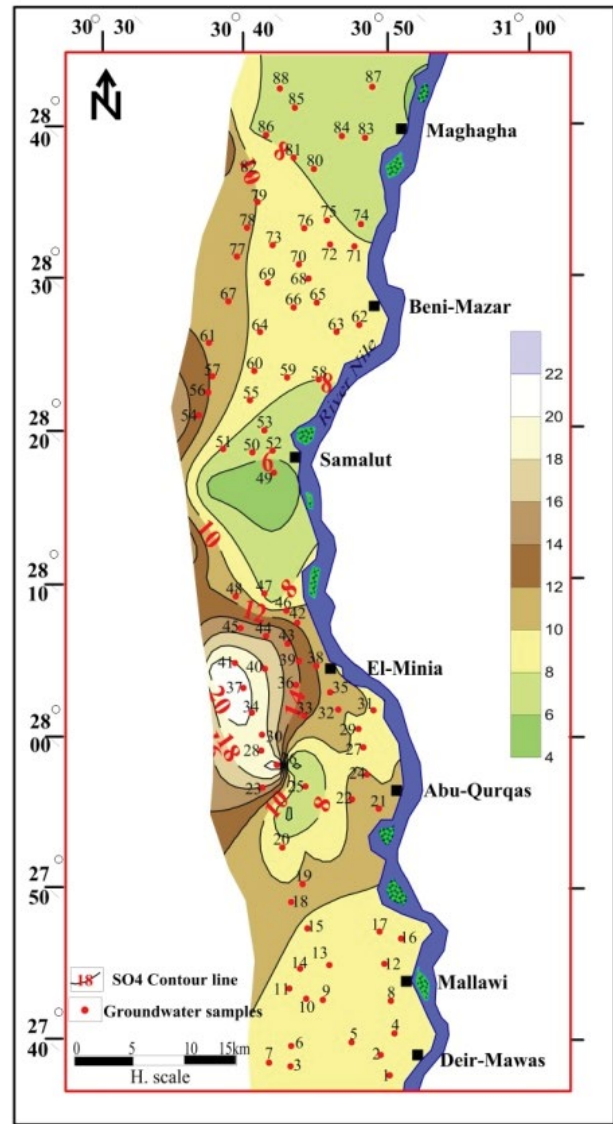
Fig. 15. Spatial distribution of SO_4^{2-} ion.

Table 4
Statistics of heavy metals concentration (all in mg/L) in studied water samples

Parameters	B	Zn	Cu	Mn	Fe	Co	Pb	Cd	Cr	As	Hg	Ni	Al	Se
Number of samples	88.00	88.00	88.00	88.00	88.00	88.00	88.00	88.00	88.00	88.00	88.00	88.00	88.00	88.00
Average	0.36	0.31	0.25	0.40	0.19	0.21	0.03	0.02	0.05	0.03	0.00	0.01	0.01	0.02
Median	0.08	0.08	0.01	0.20	0.10	0.00	0.00	0.00	0.01	0.01	0.00	0.01	0.00	0.01
Variance	0.30	0.18	0.57	0.17	0.04	0.17	0.00	0.00	0.01	0.00	0.00	0.00	0.00	0.00
Standard deviation	0.55	0.42	0.75	0.41	0.21	0.41	0.07	0.03	0.08	0.06	0.01	0.03	0.03	0.05
Minimum	0.00	0.00	0.00	0.00	0.00	0.00	0.00	0.00	0.00	0.00	0.00	0.00	0.00	0.00
Maximum	1.87	1.44	2.86	1.60	0.60	1.40	0.37	0.18	0.32	0.25	0.08	0.25	0.19	0.29
Upper quartile	0.03	0.02	0.00	0.10	0.00	0.00	0.00	0.00	0.00	0.00	0.00	0.00	0.00	0.00
Lower quartile	0.33	0.53	0.01	0.70	0.40	0.01	0.01	0.01	0.09	0.01	0.00	0.01	0.01	0.01
Inter quartile range	0.30	0.51	0.01	0.60	0.40	0.01	0.01	0.01	0.09	0.01	0.00	0.01	0.01	0.01

samples 79 and 83 stand apart, but an unambiguous explanation has not been successfully found.

Interesting facts resulting from a correlation matrix created for the data set by the UNISTAT program (see Table A1 in Appendix).The highest functional linear dependence is shown by TDS and electric conductivity ($p = 1$). This is a logical result in view of the fact that the conductivity depends on the concentration of ions in the solution and their charge and mobility. Furthermore, conductivity is also dependent on temperature, thus increases by approximately 2% EC with a temperature increase by 1°C [36], but the temperature was not taken into consideration.
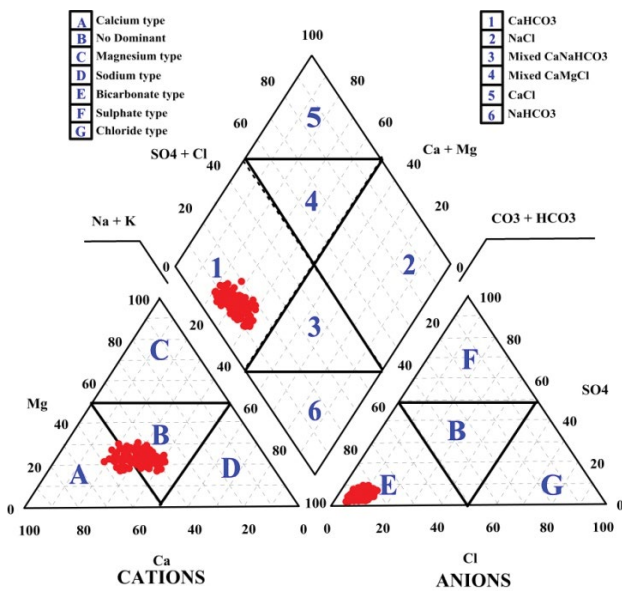
Fig. 16. Piper trilinear diagram of the studied groundwater samples.

Another high functional linear dependence is shown by carbonate components in the solution (HCO_3^-, Ca^{2+}, Mg^{2+}). The correlation coefficient has come out $p_{HCO_3/Ca} = 0.949$, or $p_{HCO_3/Mg} = 0.907$. All of these parameters are primarily dependent on conductivity, osmolality, pH, and ionic strength of the solution [37]. This is also corroborated by other high functional linear dependencies of these substances on total dissolved solids ($p_{TDS/Ca} = 0.763$; $p_{TDS/Mg} = 0.823$; $p_{TDS/HCO_3} = 0.772$) and electric conductivity ($p_{EC/Ca} = 0.763$; $p_{EC/Mg} = 0.824$; $p_{EC/HCO_3} = 0.772$) of the examined samples. The correlation does not validate any remarkable functional linear dependence of the system carbonate components on a pH of solution, which is interesting.

Based on previous information, it is possible to deduce that the carbonate reactions in the solution are primarily influenced by the substances concentration and the solution to EC.

The ion correlation Na^+ and K^+ ($p_{Na/K} = 0.790$) and Ca^{2+} and Mg^{2+} ($p_{Ca/Mg} = 0.893$) pertain to standard and expectedly high linear dependencies. This is relatively due to the identical dimensions of atomic radii and similar properties of specific elements, which in turn results in cations capable of mutual substitution in the structure of the compound.

Interesting is the high functional linear dependence of all standard major-components determined in the solution on chlorides ($p_{Ca/Cl} = 0.855$; $p_{Mg/Cl} = 0.773$; $p_{Na/Cl} = 0.833$; $p_{K/Cl} = 0.807$; $p_{HCO3/Cl} = 0.817$; $p_{SO4/Cl} = 0.871$). In natural systems, the chlorides are considered to be a conservative element, getting to the solution above all from rainfall or by mixing with seawater or fossil water; to a minimum or zero extent by rocks dissolving. Chlorine, like other halides, is very reactive. It reacts directly with most of the elements, and at a sufficient concentration in the solution, which is fulfilled in these formulas; it reacts with the elements, forming ionic compounds and complexes [38]. This probably explains the high functional linear dependence.
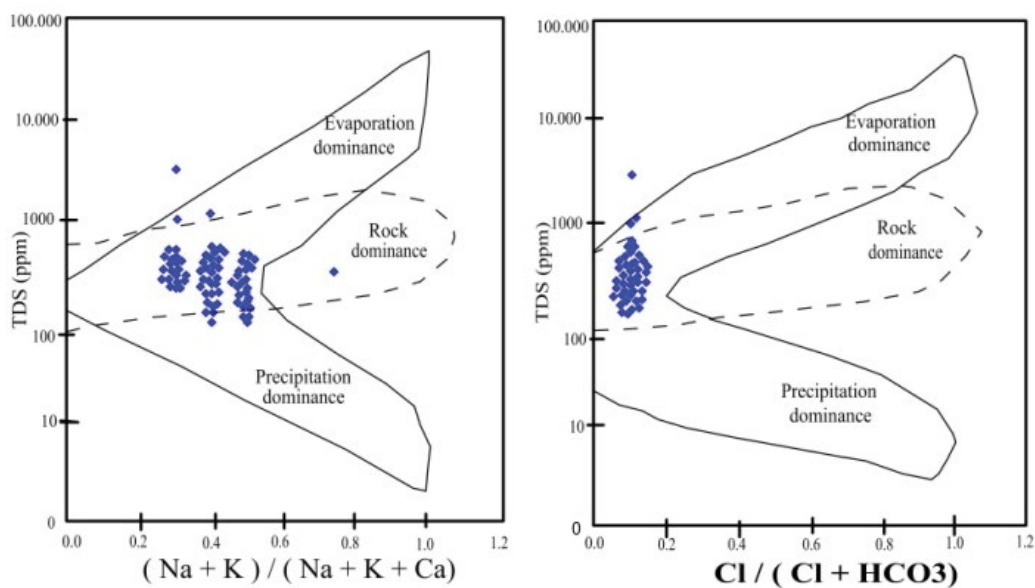
Fig. 17. Controlling mechanism of groundwater chemistry [28].

Graph of principal components
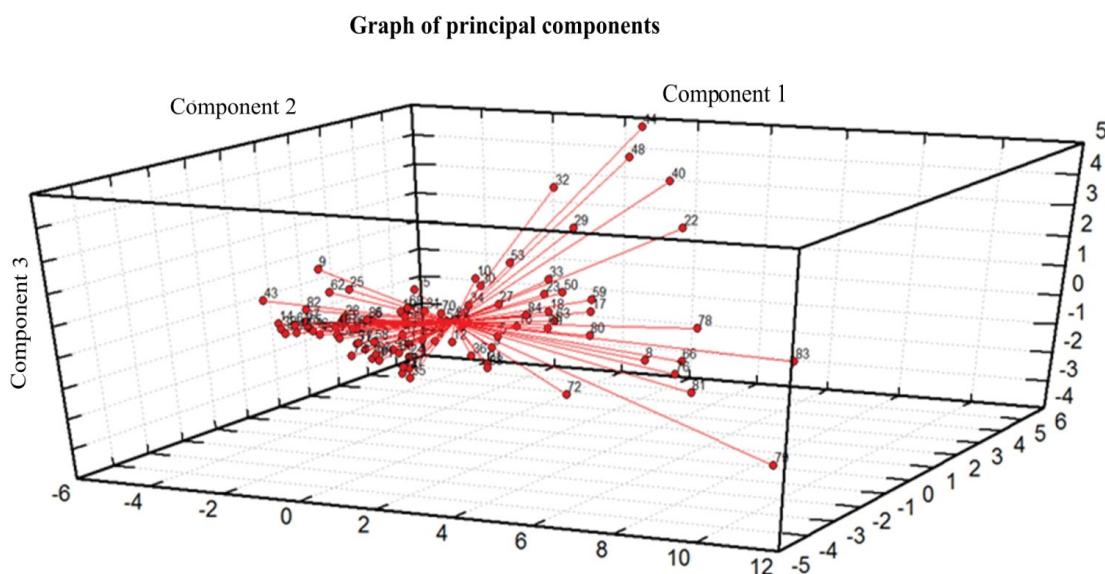
Fig. 18. PCA of hydrogeochemical data.

Table 5
Input data for equilibrium model in PHREEQC

	Average	Max.	Min.
pH	7.88	8.20	6.8
Ca^{2+}	52.86	150.00	22.8
Mg^{2+}	24.76	74.00	9.0
Na^+	29.88	82.00	20.0
K^+	3.92	12.00	2.1
HCO_3^-	299.52	850.00	138.0
SO_4^{2-}	11.21	22.00	7.0
Cl^-	32.61	70.00	16.0
B	0.36	1.87	0.083
Zn	0.34	1.44	0.075
Cu	0.25	2.86	0.003
Mn	0.53	1.60	0.000
Fe	0.28	0.60	0.000
Pb	0.03	0.37	0.009
Cd	0.02	0.18	0.007
Al	0.01	0.19	0.002

Table 6
Outputs from equilibrium models represented by saturation indices SI for average parameters and samples with maximum and minimum values of monitored parameters

Phase	log SI			Formula
	Average	Max.	Min.	
$Al(OH)_3(a)$	–2.49	–1.55		$Al(OH)_3$
Alunite	–9.72	–7.10		$KAl_3(SO4)_2(OH)_6$
Anglesite	–5.68	–5.29		$PbSO_4$
Anhydrite	–2.89	–2.41	–3.30	$CaSO_4$
Aragonite	0.45	1.51	–1.36	$CaCO_3$
Calcite	0.59	1.66	–1.23	$CaCO_3$
$Cd(OH)_2$	–4.88	–3.44		$Cd(OH)_2$
$CdSO_4$	–11.07	–10.13		$CdSO_4$
Cerussite	–0.98	0.00		$PbCO_3$
Dolomite	1.20	3.37	–2.50	$CaMg(CO_3)_2$
$Fe(OH)_3(a)$	2.29	2.61		$Fe(OH)_3$
Gibbsite	0.20	1.14	0.53	$Al(OH)_3$
Goethite	8.18	8.5		FeOOH
Gypsum	–2.67	–2.20	–3.08	$CaSO_4:2H_2O$
Halite	–7.59	–6.86	–8.09	NaCl
Hematite	18.37	19.02		Fe_2O_3
Jarosite-K	–5.30	–4.53		$KFe_3(SO4)_2(OH)_6$
Melanterite	–9.42	–9.90		$FeSO_4:7H_2O$
Otavite	0.29	1.82		$CdCO_3$
$Pb(OH)_2$	–1.68	–0.79		$Pb(OH)_2$
Siderite	–1.37	–1.27		$FeCO_3$
Smithsonite	–0.93	–0.60		$ZnCO_3$
$Zn(OH)_2(e)$	–1.84	–1.61		$Zn(OH)_2$

Moreover, high functional linear dependencies on one another have been proved in trace elements. A high correlation has especially been found out in boron with chrome ($p_{B/Cr}$ = 0.880), with cobalt ($p_{B/Co}$ = 0.773) and with lead ($p_{B/Pb}$ = 0.736). In nature, elementary boron does not occur as an element, but as a component of boric acid occurring in certain natural waters, especially in volcanic areas [39]. Widely known borate minerals include borax, kernite, and colemanite. Boron is characterized by high chemical resistance and stability. In compounds, it occurs as trivalent, rarely bivalent and monovalent. Due to its high affinity to oxygen and other electronegative elements boron can displace metals from oxides, chlorides, and sulfides under suitable

conditions. Besides, it is also capable of reacting with a series of transition metals, creating borides (e.g. Cr_5B_3) [40].

In addition, there are high correlations between both cobalt and cadmium ($p_{Co/Cd}$ = 0.754), and cobalt and chrome ($p_{Co/Cr}$ = 0.689). The correlation matrix has not proved any functional linear dependence between cobalt and nickel ($p_{Co/Ni}$ = 0.349), although, in nature, cobalt always occurs at the presence of nickel, as they can substitute for each other in certain mineral phases. The same thing applies to iron and arsenic; however, no higher functional dependence among specific elements has been proved ($p ≈ 0.5$).

3.6. Geochemical modeling in PHREEQC

Three data sets were selected for hydrogeochemical modeling in PHREEQC [27]. Two of them represented the data set with the highest and the lowest concentrations of ions, while the third data set represented the averages of parameters (Table 5). The equilibrium model for the above-mentioned data sets was calculated by PHREEQC.

As shown in Table 6, in the case of maximum values sample and average sample, the same mineral phases precipitated from the solution. The results differentiate only saturation indices SI, which provide information on how far the sample is from equilibrium. For the sample with the highest values of measured parameters, the SI is higher than it is in the average data set sample.

An interesting SI result occurs in the plumb mineral – cerussite. In the maximum sample, cerussite is in balance (SI = 0), while in the average data sample, the solution is unsaturated against cerussite (SI = –0.98). Cadmium precipitation from the solution is also very important, which is evidenced by the value SI average = 0.29, or SI max = 1.82. Cadmium (Cd) and plumb/ Lead (Pb) are among a few elements whose influence on human health and the environment is undoubtedly negative. Cd and Pb are chemically very similar to Zn. It is the very chemical similarity of these elements, which causes problems, as cadmium may easily enter various enzymatic reactions instead of zinc, and as a result, biochemical processes do not take place, or they proceed differently [41]. Another risk factor of cadmium and plumb is the fact that they are extraordinarily cumulative poisons.

The received Cd and Pb discharge from the organism only gradually, very slowly and with difficulties, and most of them concentrate on kidneys, and liver (in low amounts). It has been proved that both elements may remain in the body even for tens of years. Cadmium is evidently carcinogenic, and its high content in the organism increases the risk of cancer growth. Cadmium gets to the organism in two ways: in food and liquids, and by breathing. Thus, their precipitation from the solution reduces, in a natural way, the concentrations of these harmful substances in groundwater at the study locality. This is a positive finding affecting both the environment quality and human health.

Also, in both samples of carbonate minerals (calcite, aragonite, and dolomite) and iron, amorphous forms precipitate, which creates surface coatings and/or cement among grains in the aquifer.

Aluminum precipitates under given physical and chemical conditions in the aquifer in a crystalline form (gibbsite). In a neutral environment of common drinking water of

pH = 7, aluminum is perfectly stable and safe. A problem has occurred recently when the acidity of drinking water slightly increases, especially due to acid rain. In such an environment, aluminum gets mobile, and it may penetrate the sources of drinking water and contaminate it.

In the sample, which has shown the lowest concentrations of all monitored parameters and concurrently also the lowest pH (6.8), the model has only proved gibbsite precipitation. The other element's concentrations are so low that the monitored sample of water is unsaturated against all other elements.

In view of the fact that the redox potential was not determined on in-situ samples, or in the laboratory, it was calculated for the specific samples in the hydrochemical program "Geochemist's Workbench". The Eh and pH values, which were further used in the evaluation in Fig. 19, are summarized in Table A2 in the Appendix.

The pH value, in the sample set, ranges within the limits from 6.80 to 8.20, and the pH average value is 7.88. These values represent neutral waters (pH ≈ 7) and slightly alkaline waters (pH up to 8.3) [42]. The Eh values range is from –113 to –51, and the average Eh is –70.69. It is a slightly reducing environment, corresponding with shallow aquifers.

In the diagram shown in Fig. 19, the Eh and pH functional dependence is illustrated. As shown by the trend line, there is no linear functional dependence between the redox potential and pH.

A pH-Eh diagram for the studied system was plotted in the Geochemist Workbench hydrochemical program. The model input parameters (dominant macro-components average values) are shown in Table 5.

Afterward, the temperature of 25°C was entered into the program. The temperature was estimated since the temperature measurement was not performed in the analyzed samples. The pressure was chosen as the atmospheric pressure value ($p = 0,101$ MPa), which corresponds to shallow unconfined aquifers on the water table.

In Fig. 20, the Eh-pH diagram is presented for Ca ion of the analyzed water samples. All sampled waters were classified as waters of Ca-HCO_3 type. It is evident from the diagram that calcite precipitates in all collected water samples. This has not been proven by modeling in the PHREEQC program, whereas, in the sample with the lowest pH and the lowest concentrations of all monitored parameters, calcites do not precipitate. The reason may lie in the fact that
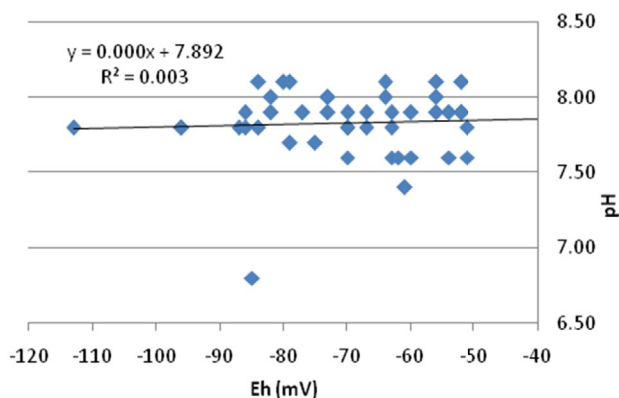
Fig. 19. Eh-pH graph for water samples.
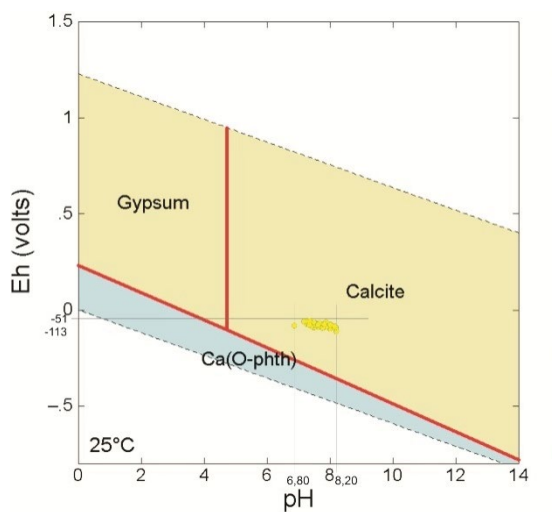
Fig. 20. Eh-pH diagram for Ca without Fe under the conditions specified in the text.
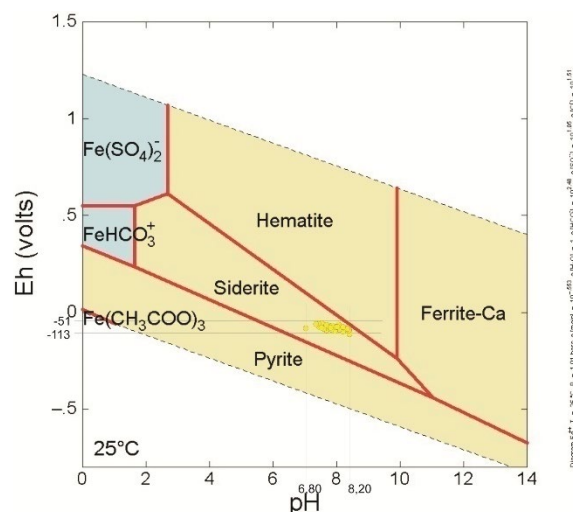
Fig. 21. Eh-pH diagram for Fe under the conditions specified in the text.

Table 7
Input parameters for pH-Eh diagram in program Geochemist Workbench, module Act 2

Ca^{2+}	HCO_3^-	SO_4^{2-}	Cl^-	Fe^{2+}
log activity				
1.723	2.476	1.048	1.513	−0.553

the data entered in the PHREEQC program did not take Eh into account, and, on the contrary, other components were entered (e.g. Fe, Al, Mn), which affected the equilibrium in solution.

In Fig. 21, there is the Eh-pH diagram for Fe. It is evident that, in the monitored samples, iron precipitates together with carbonates, which creates a dominant anion, in the form of siderite.

Finally, in Fig. 22, there is the Eh-pH diagram of Ca with Fe as per the parameters described above. Based on the diagram, the amorphous form of calciferous iron precipitates in all samples. However, only in the sample with the lowest pH calcite will precipitates from the solution under the specified conditions.

4. Conclusions

- The Quaternary aquifer represents the main aquifer in the study area; this aquifer is mainly recharged from surface water, while discharge is through evaporation processes and connection to the underlying aquifer and the River Nile.
- The alkaline earth metals (Ca^{2+} + Mg^{2+}) exceed alkali metal cations (Na^+ + K^+) and groundwater is mainly of meteoric origin.
- The multi-parametric PCA analysis shows that the set is relatively homogenous, that samples 79 and 83 stand apart, but an unambiguous explanation has not been successfully found.

Fig. 22. Eh-pH diagram for Ca with Fe under the conditions specified in the text.

- The highest functional linear dependency is shown between TDS and EC (p = 1)as well as between carbonate substances in the solution (HCO_3^-, Ca^{2+}, Mg^{2+}).The ion correlation Na^+ and K^+ ($p_{Na/K}$ = 0.790) andCa^{2+} and Mg^{2+} ($p_{Ca/Mg}$ = 0.893) pertain to standard and expectedly high linear dependencies. Moreover, high functional linear dependencies on one another have been proved in trace elements. A high correlation has especially been found out in boron with chrome ($p_{B/Cr}$ = 0.880), cobalt ($p_{B/Co}$ = 0.773) and lead ($p_{B/Pb}$ = 0.736).
- The hydrogeochemical modeling has proved that, in the max sample, cerussite is in balance (SI = 0), while the solution is unsaturated against cerussite (SI = −0.98) in the average data sample. Cadmium precipitates from the

solution, which is evidenced by the value SI max = 1.82. Cadmium and plumb are among a few elements, whose influence on human health and the environment is undoubtedly negative. Cadmium is evidently carcinogenic, and its high content in the organism increases the risk of cancer growth.

• The Eh-pH diagram for a Ca ion shows that all sampled waters are classified as Ca-HCO$_3$ water type and calcite precipitates in all collected water samples. The Eh-pH diagram of Ca with Fe proves that the amorphous form of calciferous iron precipitates in all samples. However; only in the sample with the lowest pH, calcite precipitates from the solution under specified conditions.

• Forty-nine percent (49%) of the collected groundwater samples exhibit high values of B, Mn, As, Hg, Cr, Ni, Co, Cd, and Se. These high values could be explained by the leaching of El Moheet drain which receives industrial water, drainage water of splendiferous irrigated soil and Eocene rocks; and corrosion of well casings and other pipes. However, 51 % of the groundwater samples are suitable for drinking because these elements have values below the permissible limits of Egyptian standards guidelines. In other words, 51% of the samples do meet the national drinking water standards.

• Microbiological analysis of the collected water shows that 75% are free of protozoa, Schistosoma, Minthe, and Charophyte (algae) and the rest (25%) are positive (have shown the presence of bacterial contamination) due to infiltration from septic tanks.

References

[1]	P. Li, H. Qian, Water resources research to support a sustainable China, Int. J. Water Resour. Dev., 34 (2018) 327–336.
[2]	D.K. Todd, L.W. Mays, Groundwater Hydrology, John Wiley & Sons, New York, 2005.
[3]	A. Ayman, Using generic and pesticide DRASTIC GIS-based models for vulnerability assessment of the Quaternary aquifer at Sohag, Egypt, Hydrogeology, 17 (2009) 1203–1217.
[4]	A.K. Kamel, Hydrochemical Evaluation of the Water Resources in Minia District, Egypt, M.Sc. Thesis, Geology Department, Faculty of Science, Minia University, 2012, pp. 1–16.
[5]	E. El-Sayed, M. El Kashouty, A. Kamel, The hydrochemical characteristics and evolution of groundwater and surface water in the western part of the River Nile, El-Minia district, Upper Egypt, Arabian J. Geosci., 5 (2010) 637–652.
[6]	M. El Kashouty, Modeling of the Limestone Aquifer Using Isotopes, Major and Trace Elements in the Western River Nile between Beni-Suef and El-Minia, 14th International Water Technology Conference (IWTC 14), Cairo, Egypt, 2010, pp. 1–15.
[7]	M.S. Morsi, Studied the Environmental Impact of Anthropogenic Activities on Surface and Groundwater System in the Western Part of the River Nile, Minia district, M.Sc. Faculty of Science, Geology Department, Minia University, Minia, 2012, pp. 1–15.
[8]	E. Ismail, Studied the Environmental Investigation in the West Tahta Region, Upper Egypt: Hydrochemical, Geophysical, and Remote Sensing Study, Ph.D. Thesis, Department, Angewandte Geowissenschaften Geophysik, Montanuniversitat Leoben, Austria, 2013.
[9]	R. Zaki, E.A. Ismail, W.S. Mohamed, A.K. Ali, Impact of surface water and groundwater pollutions on irrigated soil, El Minia Province, Northern Upper Egypt, J. Water Resour. Prot., 7 (2015) 1467–1472.
[10]	E. Ismail, Z. Rafat, K. Ali, Hydrogeochemistry and Evaluation of Groundwater Suitability for Irrigation and Drinking Purposes in West El-Minia District, North Upper Egypt, Proceedings of Eighteenth International Water Technology Conference, IWTC18 Sharm El-Sheikh, 2015.
[11]	A.A. Abdel Moneim, J.P. Fernández-Álvarez, E.M. Abu El Ella, A.M. Masoud, Groundwater management at West El-Minia Desert Area, Egypt using numerical modeling, J. Geosci. Environ. Prot., 4 (2016) 66–76.
[12]	E. Ismail, E. El-Sayed, S. Sakr, E. Youssef, Characteristic of groundwater potentialities in West Nile Valley South, Minia Governorate, Egypt, Arabian J. Geosci., 10 (2017) 521.
[13]	E. Ismail, M. El-Rawy, Assessment of groundwater quality in West Sohag, Egypt, Desal. Water Treat., 123 (2018) 101–108.
[14]	A. Abdelhalim, A. Sefelnasr, E. Ismail, Numerical modeling technique for groundwater management in Samalut city, Minia Governorate, Egypt, Arabian J. Geosci.,12 (2019) 124.
[15]	A.E. Farag, M.D. Ahmed, M.H. El-Sayed, Evaluation of water resources in El-Minya governorate, Egypt for drinking and irrigation purposes, Environ. Sci. Indian J., 4 (2009) 138–152.
[16]	M. El-Rawy, E. Ismail, O. Abdalla, Assessment of groundwater quality using GIS, hydrogeochemistry, and factor statistical analysis in Qena governorate, Egypt, Desal. Water Treat., 162 (2019) 14–29.
[17]	M.G. Snousy, E. Ismail, R. Zaki, Trace element occurrence and distribution problems in the irrigation water at El-Minia district, north Upper Egypt, Arabian J. Geosci., 12 (2019) 582.
[18]	G. Yasmin, D. Islam, M.T. Islam, M. Shariot-Ullah, A.K.M. Adham, Evaluation of groundwater quality for irrigation and drinking purposes in Barisal district of Bangladesh, Fund. Appl. Agric., 4 (2019) 632–641.
[19]	A.K. Rasul, Hydrochemistry and quality assessment of Derbendikhan Reservoir, Kurdistan Region, Northeastern Iraq, Arabian J. Geosci., 12 (2019) 312.
[20]	P. Li, R. Tian, R. Liu, Solute geochemistry and multivariate analysis of water quality in the Guohua Phosphorite Mine, Guizhou Province, China, Exposure Health, 11 (2019) 81–94.
[21]	P. Li, J. Wu, R. Tian, S. He, X. He, C. Xue, K. Zhang, Geochemistry, Hydraulic connectivity and quality appraisal of multilayered groundwater in the Hongdunzi coal mine, Northwest China, Mine Water Environ., 37 (2018) 222–237.
[22]	A.D. Eaton, L.S. Clesceri, A.E. Greenberg, Standard Methods for the Examination of Water and Wastewater, 20th ed., American Public Health Association (APHA), AWWA, WPCF, New York, 2005.
[23]	A. Bozdag, Combining AHP with GIS for assessment of irrigation water quality in Çumra irrigation district (Konya), Central Anatolia, Turkey, Environ. Earth Sci., 73 (2015) 8217–8236.
[24]	S. Singh, N.J. Raju, C. Ramakrishna, Evaluation of groundwater quality and its suitability for domestic and irrigation use in parts of the Chandauli-Varanasi region, Uttar Pradesh, India, J. Water Resour. Prot., 7 (2015) 572–587.
[25]	WHO, Guidelines for Drinking Water Quality, Volume 1: Recommendations, 4th ed., World Health Organization, Geneva, 2011.
[26]	EHCW, Egyptian Standards for Drinking Water and Domestic Uses (in Arabic), Egyptian Higher Committee for Water, 2007.
[27]	D.L. Parkhurst, C.A.J. Appelo, User's Guide to PHREEQC (Version 2)-A Computer Program for Speciation, Batch-Reaction, One-Dimensional Transport, and Inverse Geochemical Calculations, United States Geological Survey Earth Science Information Center, Denver, 1999.
[28]	R. Said, The Geology of Egypt, Balkema Publication, Rotterdam, 1990.

[29] R. Zaki, A. El Bakry, A. El Shemi, A.F. Fanous, Petrography and Geochemistry of the Eocene Limestone Units, East El-Minia district, North Upper Egypt, Proceedings of 5th International Conference on Geochemistry, Alexandria University, Egypt, II2010, pp.113–148.

[30] M.A. Tamer, M. El-Shazly, A. Shata, Geology of El-Fayum, Beni-Suef regions, Bull. Desert Inst. Egypt, 24 (1974) 1–30.

[31] RIGW, Hydrogeological Map of Egypt, Scale 1:100000, 2nd ed., Map Sheet of El-Minia, Research Institute for Groundwater, 1992.

[32] J.D. Hem, Study and Interpretation of the Chemical Characteristics of Natural Water, United States Geological Survey, Water Supply, Paper 2254, Washington DC, 1985, pp. 23–25.

[33] A.M. Piper, A Graphic Procedure in the Geo-Chemical Interpretation of Water Analysis, USGS Groundwater Note, 1953, pp. 1–12.

[34] R.J. Gibbs, Mechanism controlling world water chemistry, Science, 170 (1970) 1088–1090.

[35] J. Wu, P. Li, D. Wang, X. Ren, M. Wei, Statistical and multivariate statistical techniques to trace the sources and affecting factors of groundwater pollution in a rapidly growing city on the Chinese Loess Plateau, Hum. Ecol. Risk Assess. Int. J., (2019), https://doi.org/10.1080/10807039.2019.1594156.

[36] C.E. Boyd, Water Quality: An Introduction, Springer International Publishing, 2020.

[37] W.B. White, Geomorphology and Hydrology of Karst Terrains, Oxford University Press, New York, 1988.

[38] T.J. Jentsch, V. Stein, F. Weinreich, A.A. Zdebik, Molecular structure and physiological function of chloride channels, Physiol. Rev., 82 (2002) 503–568.

[39] C.A.J. Appelo, D. Postma, Geochemistry, Groundwater and Pollution, 2nd ed., A.A. Balkema Publishers, Leiden, 2005.

[40] J.I. Drever, The Geochemistry of Natural Waters, Surface and Groundwater Environment, 3rd ed., Prentice-Hall, New Jersey, 1997.

[41] R. Carballo, A. Castiñeras, A. Domínguez-Martin, I. García-Santos, J. Niclós-Guttiérrez, Solid-State Structures of Cadmium Complexes with Relevance to Biological Systems, A. Sigel, H. Sigel, R.K.O. Sigel, Eds., Cadmium: From Toxicology to Essentiality, Metal Ions in Life Sciences, 11. Springer, 2013, pp.145–189.

[42] W. Stumm, J.J. Morgan, Aquatic Chemistry: Chemical Equilibria and Rates in Natural Waters, 3rd ed., John Wiley and Sons, New York, 1996.

Appendix

Table A1
Correlation matrix of hydrogeochemical data

	EC	pH	TDS	Ca²⁺	Mg²⁺	Na⁺	K⁺	HCO₃⁻	SO₄²⁻	Cl⁻	B	Zn	Cu	Mn	Fe	Co	Pb	Cd	Cr	As	Hg	Ni	Al	Se
EC	1.000																							
pH	0.499	1.000																						
TDS	1.000	0.499	1.000																					
Ca²⁺	0.763	0.345	0.763	1.000																				
Mg²⁺	0.824	0.408	0.823	0.893	1.000																			
Na⁺	0.616	0.312	0.616	0.710	0.745	1.000																		
K⁺	0.685	0.307	0.685	0.787	0.750	0.790	1.000																	
HCO₃⁻	0.571	0.319	0.572	0.640	0.580	0.707	0.720	1.000																
SO₄²⁻	0.557	0.291	0.558	0.659	0.591	0.714	0.749	0.647	1.000															
Cl⁻	0.702	0.361	0.702	0.855	0.773	0.833	0.807	0.817	0.871	1.000														
B	0.205	0.195	0.205	0.044	0.101	0.026	0.022	0.082	0.035	0.052	1.000													
Zn	0.003	0.017	0.003	-0.006	-0.077	0.083	0.063	-0.023	0.154	0.134	0.572	1.000												
Cu	0.006	0.097	0.006	-0.126	-0.034	-0.083	-0.061	-0.114	-0.103	-0.071	0.568	0.269	1.000											
Mn	0.216	0.091	0.216	0.208	0.134	0.309	0.286	0.159	0.362	0.382	0.315	0.361	0.082	1.000										
Fe	0.153	0.174	0.153	0.132	0.045	0.068	0.016	0.080	0.084	0.148	0.463	0.236	0.168	0.625	1.000									
Co	0.100	0.067	0.100	0.033	0.024	0.003	-0.079	0.024	-0.042	0.023	0.773	0.545	0.448	0.352	0.494	1.000								
Pb	0.206	0.152	0.206	0.049	0.141	-0.001	-0.017	0.094	-0.078	-0.028	0.736	0.300	0.620	0.118	0.227	0.591	1.000							
Cd	0.103	0.048	0.103	-0.043	-0.001	-0.040	-0.099	-0.046	-0.050	-0.024	0.670	0.377	0.621	0.224	0.269	0.754	0.683	1.000						
Cr	0.134	0.144	0.134	0.015	0.036	0.021	0.017	0.033	0.046	0.038	0.880	0.516	0.414	0.385	0.456	0.689	0.610	0.558	1.000					
As	0.038	0.054	0.038	-0.134	-0.068	-0.018	-0.017	-0.100	-0.041	-0.021	0.536	0.593	0.500	0.264	0.228	0.436	0.375	0.505	0.490	1.000				
Hg	0.026	-0.010	0.026	-0.044	-0.030	0.057	0.192	-0.036	0.135	0.063	0.138	0.264	0.276	0.069	-0.106	-0.069	-0.042	0.003	0.230	0.383	1.000			
Ni	0.041	0.095	0.042	-0.069	-0.094	0.005	-0.046	-0.088	0.079	0.007	0.350	0.338	-0.023	0.245	0.237	0.349	-0.022	0.122	0.373	0.035	0.069	1.000		
Al	0.121	0.195	0.121	0.034	0.078	-0.019	0.015	0.063	-0.014	0.032	-0.004	-0.129	-0.095	0.023	0.091	0.013	0.009	-0.057	0.074	0.036	-0.050	0.022	1.000	
Se	0.031	0.074	0.031	-0.025	-0.069	0.015	-0.025	-0.057	0.075	0.088	0.326	0.357	0.127	0.309	0.285	0.361	0.018	0.219	0.406	0.158	0.159	0.439	0.017	1.000

Table A2
Measured pH and calculated values of Eh for individual samples

No.	Eh	pH	No.	Eh	pH	No.	Eh	pH	No.	Eh	pH
1	–67	7.80	23	–70	7.90	45	–74	7.70	67	–54	8.00
2	–63	7.60	24	–84	8.10	46	–84	7.80	68	–56	7.90
3	–86	7.90	25	–75	7.70	47	–75	8.10	69	–52	8.20
4	–82	7.90	26	–96	7.80	48	–96	8.10	70	–79	7.90
5	–73	7.90	27	–64	8.00	49	–60	7.90	71	–75	7.90
6	–70	7.60	28	–70	7.80	50	–54	7.60	72	–96	7.80
7	–54	7.60	29	–87	7.80	51	–54	8.00	73	–73	7.80
8	–70	7.80	30	–77	7.90	52	–56	7.80	74	–74	7.90
9	–62	7.60	31	–60	7.90	53	–55	7.70	75	–84	8.00
10	–54	7.90	32	–56	7.90	54	–77	8.10	76	–54	8.10
11	–51	7.80	33	–63	7.80	55	–61	8.10	77	–63	7.90
12	–64	8.10	34	–67	7.90	56	—56	7.90	78	–60	8.10
13	–113	7.80	35	–86	7.80	57	–52	8.20	79	–76	8.20
14	–60	7.60	36	–82	8.00	58	–79	7.80	80	–99	8.00
15	–51	7.60	37	–96	7.80	59	–63	7.90	81	–85	7.90
16	–52	8.10	38	–84	7.80	60	–85	8.00	82	–54	7.60
17	–56	8.00	39	–56	8.10	61	–73	7.60	83	–79	8.20
18	–52	7.90	40	–52	7.90	62	–74	7.70	84	–75	7.90
19	–79	7.70	41	–79	8.10	63	–84	7.80	85	–96	8.10
20	–61	7.40	42	–63	7.90	64	–75	7.80	86	–56	8.10
21	–80	8.10	43	–85	6.80	65	–96	7.70	87	–52	7.90
22	–73	8.00	44	–73	8.00	66	–60	8.10	88	–88	8.00